LBL-12642
Preprint

Lawrence Berkeley Laboratory
UNIVERSITY OF CALIFORNIA

Submitted to Nuclear Physics A

THE DYNAMICS OF THE FUSION OF TWO NUCLEI

W. J. Swiatecki

April 1981

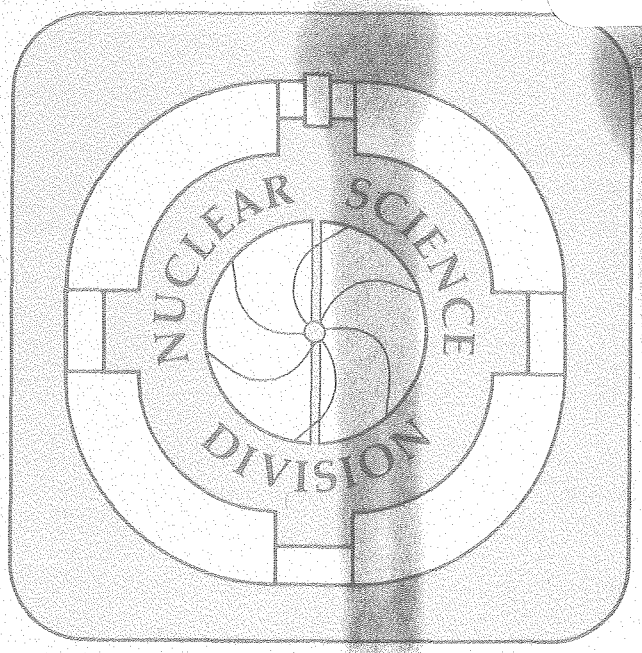

Prepared for the U.S. Department of Energy under Contract W-7405-ENG-48

DISCLAIMER

LBL-12642

THE DYNAMICS OF THE FUSION OF TWO NUCLEI

W.J. Swiatecki

Nuclear Science Division
Lawrence Berkeley Laboratory
University of California
Berkeley, CA 94720

April 1981

This work was supported by the Director, Office of Energy Research, Division of Nuclear Physics of the Office of High Energy and Nuclear Physics of the U.S. Department of Energy under Contract W-7405-ENG-48.

LBL-12642

THE DYNAMICS OF THE FUSION OF TWO NUCLEI

W.J. Swiatecki

Nuclear Science Division
Lawrence Berkeley Laboratory
University of California
Berkeley, CA 94720

April 1981

The prediction of the need for an extra push over the interaction barrier in order to make the heavier nuclei fuse is made the basis of a simple algebraic theory for the energy-dependence of the fusion cross-section. The predictions are compared with recent experiments. A graphical construction, designed to extract directly the three parameters of the theory, suggests about 33 for the effective fissility $(Z^2/A)_{eff}$ [defined as $4Z_1Z_2/A_1^{1/3}A_2^{1/3}(A_1^{1/3} + A_2^{1/3})$] beyond which an extra push is needed, determines the initial rate of increase of the square root of the extra push (in MeV) as about one per unit excess of $(Z^2/A)_{eff}$ over 33 and indicates an effective centrifugal repulsion opposing fusion (in cases when angular momentum is present) not very different from that expected for two spheres rolling on each other without sliding.

I. INTRODUCTION

It is obvious that after two nuclei have been brought into contact (using a center-of-mass energy corresponding to the interaction barrier) the further time evolution of the system (either towards fusion or reseparation) will be governed by the relative magnitudes of the repulsive electric forces and the cohesive nuclear forces. For light systems, for which the electric forces are small, the configuration of tangent nuclei would be expected to evolve automatically towards a fused system. For heavier nuclei, the electric repulsion may become so large that, starting from rest at contact, the system will reseparate, the dynamical evolution taking place entirely outside that critical saddle-point in configuration space which has to be overcome in order to make a fused system. In those cases an additional bombarding energy in excess of the interaction barrier--an "extra push"--will be needed to achieve fusion.

II. THE ONE-BODY DISSIPATION DYNAMICS

These qualitative expectations were analyzed[1,2] using a schematic model, incorporating a macroscopic potential energy (the sum of electrostatic and surface energies) and the macroscopic One-body Nuclear Dissipation Function (in the form of the wall or wall-and-window formula[1-3]).

A result of that study, which follows largely on dimensional grounds (given the structure of the nuclear dynamics defined by the above ingredients, together with an approximation exploiting the relative smallness of the neck between the two nuclei) is that the extra push E in a head-on collision should have the following approximate appearance:

$$\Delta E = \left\{ \begin{array}{l} 0, \text{ for } (Z^2/A)_{\text{eff}} \leqslant (Z^2/A)_{\text{eff thr}} \\ K[(Z^2/A)_{\text{eff}} - (Z^2/A)_{\text{eff thr}}]^2 + \text{higher} \\ \qquad \text{powers of the square bracket,} \\ \qquad \text{for } (Z^2/A)_{\text{eff}} > (Z^2/A)_{\text{eff thr}} \ , \end{array} \right\} \tag{1}$$

where

$$K = \frac{A_1^{1/3}A_2^{1/3}(A_1^{1/3}+A_2^{1/3})^2}{A_1+A_2} \frac{32}{2025}\left(\frac{3}{\pi}\right)^{2/3}\left(\frac{e^2}{\hbar c}\right)^2 mc^2 \cdot a^2 \ , \tag{2}$$

with

$$(Z^2/A)_{\text{eff}} \equiv 4Z_1Z_2/A_1^{1/3}A_2^{1/3}(A_1^{1/3} + A_2^{1/3}) \ . \tag{3}$$

In the above, Z_1, Z_2, A_1, A_2 are the atomic and mass numbers of the colliding nuclei, m is the nuclear mass unit (taken as 931 MeV/c^2) and $(Z^2/A)_{\text{eff thr}}$ and $\underline{a}$ are numerical constants, to be deduced either from experiment or calculated from a given model. (The schematic model underlying Ref. (1) suggested ballpark values $(Z^2/A)_{\text{eff thr}} \approx 26\text{-}27$ and $\underline{a} \approx 5$. The analysis, given below, of the experimental evidence from Ref. (4) suggests $(Z^2/A)_{\text{eff thr}} \approx 33$ and $\underline{a} \approx 12$.]

An approximate generalization of eq. (1) to noncentral collisions is obtained by adding to the electric repulsion an effective centrifugal force [obtained from a centrifugal potential, taken as the square of the angular momentum divided by twice an effective moment of inertia--see Refs. (1,2,5) and, especially, Ref. (4)].

The kinetic energy excess in the radial (or approach) degree of freedom, i.e. the radial injection energy E_r over the interaction barrier E_B, necessary to overcome the saddle point, is then found to be given by

$$E_r = \begin{cases} 0, \text{ for } (Z^2/A)_{eff} + (L/L_{ch})^2 \leqslant (Z^2/A)_{eff\ thr} \\ K[(Z^2/A)_{eff} + (L/L_{ch})^2 - (Z^2/A)_{eff\ thr}]^2 + \cdots, \\ \qquad \text{for } (Z^2/A)_{eff} + (L/L_{ch})^2 \geqslant (Z^2/A)_{eff\ thr} \end{cases} \qquad (4)$$

where L is the angular momentum and L_{ch} is a constant (a characteristic angular momentum) given by

$$L_{ch} = \frac{e\sqrt{mr_o}}{2f} \frac{A_1^{2/3}A_2^{2/3}(A_1^{1/3}+A_2^{1/3})}{\sqrt{A_1+A_2}} \quad . \qquad (5)$$

In the above, r_o is the nuclear radius constant and the quantity f is the "angular momentum fraction", i.e. that fraction of the total angular momentum which is responsible for the centrifugal force in the separation degree of freedom. This force, along with the electric repulsion, opposes capture inside the saddle-point and calls for an increased injection energy according to eq. (4). (For approaching nuclei, up to the moment of contact, f = 1. For two spheres rolling on each other without sliding f = 5/7. For rigidly stuck spheres one finds

$$f^{-1} = 1 + \frac{2}{5}\frac{1+\alpha}{\alpha}\frac{1+\alpha^{5/3}}{(1+\alpha^{1/3})^2} \quad , \text{ where } \alpha = A_2/A_1 \quad . \qquad (6)$$

This gives f = 0.54 in the case A_1 = 208 and A_2 = 50, for example).

According to the dissipation-dominated dynamics of Refs. (1,2,3), most of the extra energy over the interaction barrier is dissipated in a "thud" and a "clutch" as the two colliding nuclei are almost brought to relative rest by the strong one-body dissipation. The rapid increase in the extra injection energy with excess of $(Z^2/A)_{eff}$ over the threshold condition leads to a "thud wall" opposing the formation of composite or compound

systems in the case of collisions between heavier nuclei, characterized by values of $(Z^2/A)_{eff}$ exceeding substantially the threshold value. We shall refer to K as the "thud wall stiffness coefficient". It is numerically equal to the magnitude of the extra push (in MeV) needed when the threshold value $(Z^2/A)_{eff\ thr}$ is exceeded by one unit. The related constant a (independent of A_1 and A_2) will be called the "thud wall slope coefficient".

Equation (4), when combined with the equations of conservation of energy and angular momentum, leads to a simple formula for the fusion cross-section σ. Thus, conservation of the original (center-of-mass) energy E up to the moment of contact states that

$$E = E_B + E_r + E_t \quad , \tag{7}$$

where E_t is the tangential (or orbital) energy at, or just before, contact, given by

$$E_t = L^2/2Mr_c^2 \quad , \tag{8}$$

Here M is the reduced mass and r_c is the distance between the nuclear mass centers when the nuclei are about to touch. In the idealization where the diffuseness of the nuclear surfaces is neglected, r_c is the sum of the two nuclear radii. With diffuseness taken into account, r_c will, in general, exceed the sum of the radii by a small amount which may, moreover, depend somewhat on angular momentum.

Since angular momentum is conserved, the following expression for L is also valid:

L = M(initial relative velocity)(impact parameter b),

or

$$b^2 = \frac{L^2}{2ME} = r_c^2 \frac{E_t}{E} \quad . \tag{9}$$

Using for E_r in eq. (7) the expression (4), which gives the least radial energy needed for fusion, leads to the following equation for the fusion cross-section σ:

$$\sigma = \pi b^2 = r_c^2 \frac{E_t}{E} \quad , \tag{10}$$

where E_t is related to E by

$$E = E_B + E_t + (c_1 + c_2 E_t)^2 + \ldots \quad , \tag{11}$$

with

$$c = \sqrt{K}[(Z^2/A)_{eff} - (Z^2/A)_{eff\ thr}] \quad , \tag{12}$$

$$c_2 = \frac{\sqrt{K}}{e^2/r_o} \frac{8f^2}{A_1^{1/3} A_2^{1/3}} \quad . \tag{13}$$

Let us denote by Σ the "energy-weighted reduced cross-section", i.e. the cross-section in units of πr_c^2, multiplied by the center-of-mass energy E (so that numerically Σ is, in fact, equal to the tangential or orbital energy E_t):

$$\Sigma \equiv \frac{\sigma E}{\pi r_c^2} \quad .$$

We may now consider eqs. (10) and (11) as defining the following relation between cross-section and center-of-mass energy:

$$E = E_B + \Sigma \quad , \text{ for } c_1 + c_2 \Sigma < 0 \quad , \tag{14}$$

$$E = E_B + \Sigma + (c_1 + c_2\Sigma)^2 + \text{higher powers of the expression in brackets}$$

$$= (E_B + c_1^2) + (2c_1c_2 + 1)\Sigma + c_2^2\Sigma^2 + \ldots \quad ,$$

$$\text{for } c_1 + c_2\Sigma > 0 \quad . \tag{15}$$

Equation (14) is clearly equivalent to the standard result for the reaction cross-section, viz.:

$$\sigma = \pi r_c^2 \left(1 - \frac{E_B}{E}\right) \quad . \tag{16}$$

When $c_1 < 0$ (i.e. for systems with $(Z^2/A)_{eff} < (Z^2/A)_{eff\ thr}$) this expression holds until an energy defined by

$$c_1 + c_2\Sigma = 0 \quad , \tag{17}$$

i.e. $$c_1 + c_2(E - E_B) = 0 \quad . \tag{18}$$

Thus, the deviation from the standard formula sets in when the energy E exceeds the barrier E_B by $(-c_1)/c_2$. When $c_1 > 0$, the cross-section implied by eq. (15) is zero until the energy has exceeded the barrier E_B by c_1^2 (see Fig. 1).

Calling the deviation $\Sigma_o - \Sigma$ of the observed energy-weighted reduced cross-section from the standard result, $\Sigma_o = E - E_B$, the "cross-section defect", the content of eq. (15) may be stated in the following compact Extra Push Theorem:

"When an extra radial injection energy is needed for fusion, the square root of the cross-section defect should be approximately linear when plotted against the energy-weighted reduced cross-section , viz.

$$\sqrt{E - E_B - \frac{E\sigma}{\pi r_c^2}} = c_1 + c_2\Sigma + \ldots \quad ." \tag{19}$$

Thus, by plotting the square root of the experimental values of $E - E_B - \frac{E\sigma}{\pi r_c^2}$ versus $\frac{E\sigma}{\pi r_c^2}$, one should find, approximately, a straight line,

with intercept c_1 and slope c_2. According to eqs. (12,13) this should then enable one to deduce the effective angular momentum fraction f and the thud wall stiffness coefficient K, from which follows the thud wall slope coefficient a.

III. COMPARISON WITH EXPERIMENT

A series of recent experiments[4] appear to be in line with the expectations described in Refs. (1,2) and have already been compared[4] with numerical calculations incorporating the extra push theory, generalized for the presence of angular momentum. In what follows we shall make a similar comparison with the algebraic theory described in Section II, making use, in particular, of the graphical method for deducing the values of the parameters.

Figure 2 displays cross-sections for seven pairs of nuclei: $^{208}Pb + {}^{26}Mg$, ^{27}Al, ^{48}Ca, ^{50}Ti, ^{52}Cr, ^{58}Fe, ^{64}Ni. (The projectile was always ^{208}Pb.) The experimental points refer to cross-sections for making a fused system that disintegrates with a mass distribution of the fragments centered around symmetry (as contrasted with deep-inelastic nonfusion processes, where the mass distributions are centered around the entrance channel). These fused systems could be either true compound nuclei, trapped inside the true saddle point, or composite nuclei, also called mononuclei[1]. They are nuclear configurations without a pronounced neck, trapped inside the conditional saddle but not inside the true saddle. [A conditional saddle is a saddle at frozen (entrance channel) asymmetry[1,2].] The solid lines in Fig. 2 correspond to the standard reaction cross-section formula, eq. (16). The dashed lines result from solving eq. (15) for σ, viz.:

$$\sigma = \frac{\pi r_c^2}{E}\left[\sqrt{\left(\frac{c_1c_2+1/2}{c_2^2}\right)^2 - \left(\frac{c_1^2+E_B-E}{c_2^2}\right)} - \left(\frac{c_1c_2+1/2}{c_2^2}\right)\right] \quad , \tag{20}$$

with c_1, c_2 given by eqs. (12,13).

In making the plots in Fig. 2, the interaction barrier E_B in eq. (20) was calculated by reducing by 4% the maximum in the sum of the nuclear proximity interaction from Ref. (6) and a point-charge Coulomb interaction energy. [Figure 5 in Ref. (7) suggests that such a reduction of the proximity barriers by 4 ± 4% is needed to reproduce measured values throughout the periodic table. This 4% reduction seems also to be just what is needed to account accurately for the thresholds in the ^{26}Mg and ^{27}Al reactions in Fig. 2.]

An effective sharp contact distance r_c was chosen according to

$$r_c = C_1 + C_2 + 1.14 \text{ fm} \quad , \tag{21}$$

where C_1 and C_2 are the central radii of the nuclei, calculated according to Ref. (6), viz.:

$$C = R - \frac{1 \text{ fm}^2}{R} \quad ,$$

$$R = 1.28\, A^{1/3} - 0.76 + 0.8\, A^{-1/3} \text{ fm} \quad . \tag{22}$$

The constant 1.14 fm, which allows roughly for the diffuseness of the nuclear surfaces, was chosen to reproduce the initial slopes of the cross-section function for the ^{26}Mg and ^{27}Al reactions.

The three parameters entering the cross-section formula through eqs. (12,13) were fixed at $(Z^2/A)_{\text{eff thr}} = 33$, $\underline{a} = 12$, $f = 3/4$, by the method outlined in Section II. Thus we may rewrite eq. (19) as

$$F(X,Y) = a.Y + af^2.X \quad , \tag{23}$$

where

$$F = \frac{45}{4\sqrt{2}} \left(\frac{\pi}{3}\right)^{1/3} \left(\frac{\hbar c}{e^2}\right) \frac{1}{\sqrt{mc^2}} \frac{\sqrt{A_1+A_2}}{(A_1A_2)^{1/6}(A_1^{1/3}+A_2^{1/3})} \sqrt{E - E_B - \Sigma} \quad , \tag{24}$$

$$X = \frac{8r_o}{e^2(A_1A_2)^{1/3}} \Sigma \quad , \tag{25}$$

$$Y = (Z^2/A)_{eff} - (Z^2/A)_{eff\ thr} \quad . \tag{26}$$

Figure 3a shows the measured values of F, proportional to the square root of the cross-section defect, plotted against the measured values of X, for the seven reactions under discussion, with seven different values of Y. (Experimental points which correspond to cross-section defects that are essentially zero within the uncertainties of the analysis have been omitted in order not to clutter up the figure.) The straight lines, with slopes equal to af^2, correspond to the theoretical formula. Figure 3b shows the calculated intercepts F(0,Y) plotted versus $(Z^2/A)_{eff}$. The slope of the line in Fig. 3b gives directly the thud wall slope coefficient a, and the intercept gives $(Z^2/A)_{eff\ thr} = 33$, marked by a star.

A change in $(Z^2/A)_{eff\ thr}$, with a and f fixed, would move the line in Fig. 3b to the left or to the right, displacing the intercepts F(0,Y) in Fig. 3a up or down by equal amounts, so that the pattern of straight lines in Fig. 3a would move up and down as a rigid set. Keeping $(Z^2/A)_{eff\ thr}$ and a fixed and changing f would keep the intercepts F(0,Y) in Fig. 3a (the dots on the F-axis) fixed and pivot the lines about those points, while preserving their parallelism. Finally, changing a while keeping $(Z^2/A)_{eff\ thr}$ and f fixed would pivot the straight line in Fig. 3b about the intercept marked by a star, thus stretching or compressing the pattern of intercepts (dots) in Fig. 3a, while at the same time also pivoting each line in Fig. 3a about its intercept.

The correspondence between theory and experiment in Fig. 3a is far from perfect (though the not inconsiderable uncertainties in the measured cross-section defects should be kept in mind--see also Fig. 2). However, the overall fit seems adequate to suggest the following values for the three parameters of the theory: $(Z^2/A)_{\text{eff thr}} \approx 33 \pm 1$, $\underline{a} \approx 12 \pm 2$ and $f \approx 3/4 \pm 10\%$. (The assigned uncertainties are subjective estimates, which assume that the deviations between theory and experiment are due to imperfections in the measurements and the simplified analysis and not to a gross failure in the interpretation of the observed cross-sections).

Of the seemingly significant deviations between theory and experiment we might note the following. In the case of $^{26}Mg + ^{208}Pb$ the trend of the experimental points shows no indication of the flattening out of the cross-sections predicted by theory (although lowering only one of the experimental points by not much more than its estimated uncertainty would remove this discrepancy). In the case of $^{48}Ca + ^{208}Pb$ the experimental points are systematically higher, and in the case of $^{50}Ti + ^{208}Pb$ they are systematically lower than the theory. In the case of $^{64}Ni + ^{208}Pb$ the two high-energy points are considerably lower than theory. This might well be associated with the neglect of the higher powers in eq. (19), which would bring the calculated curve down significantly at these high values of $(Z^2/A)_{\text{eff}} + (L/L_{ch})^2$--see Fig. 11 in Ref. (1).

IV. DISCUSSION

Is it really true that the principal features of the cross-section for the fusion of two nuclei can be understood in terms of the simple algebraic model underlying Ref. (1)? Does this really imply that the essential condition for fusion is the overcoming of a conditional saddle at frozen entrance-channel asymmetry, that this saddle can be estimated by

a macroscopic treatment of the potential energy and that the time evolution of the nuclear shapes follows approximately the One-Body Dissipation Dynamics in the window and wall-and-window idealizations, according to which the two nearly spherical nuclei thud and clutch, assuming something like a rolling motion while attempting to overcome the saddle-point in configuration space?

It is clear that there are substantial uncertainties in the degree of correspondence between theory and experiment and in the significance of this correspondence. It will surely be some time before the above questions can be answered with any degree of confidence. Clearly, much further work remains to be done both experimentally and theoretically.

On the experimental side it would be well to extend the measurements in several ways. In the case of ^{26}Mg and ^{27}Al the investigation of the center-of-mass energy range between 150 and 250 MeV would be particularly instructive. The addition of several targets between ^{27}Al and ^{48}Ca and the rechecking of the ^{48}Ca and ^{50}Ti cross-sections seems indicated. The ^{58}Fe and, especially, the ^{64}Ni measurements call for several more experimental points. Targets beyond ^{64}Ni would be of considerable interest in checking on the expected steepening-up of the thud wall with increasing values of $(Z^2/A)_{eff} + (L/L_{ch})^2$.

On the theoretical side the outstanding need is to go beyond the schematic model underlying Ref. (1). That model was designed to bring out the essential algebraic structure of the theory, and this called for extreme simplifications, which quite drastically sacrificed some well-known and important quantitative aspects of the problem. (In particular, the accurately known macroscopic saddle-point shapes and energies were replaced by schematic approximations.) An improvement of these quantitative aspects

of the theory is possible along the lines of Ref. (8). This would sharpen up the conclusions one could draw from the confrontation of theory and experiment. A concrete question of particular interest is whether the three parameters of the present theory, as deduced from fits to experiment, can be understood quantitatively from first principles. The following observations may be relevant in this connection.

A. The Threshold Fissility $(Z^2/A)_{\text{eff thr}}$

As regards the value $(Z^2/A)_{\text{eff thr}} \approx 33 \pm 1$, the sense of the deviation of this result from the value 26-27, suggested in Ref. (1), is readily understood in terms of the deviations of the schematic saddle-point shapes underlying Ref. (1) from the exact macroscopic saddles. To appreciate this, recall that the physical reason for the existence of a threshold value of $(Z^2/A)_{\text{eff}}$ is that for a system with $(Z^2/A)_{\text{eff}}$ greater than about the threshold value the conditional saddle-point configuration becomes more compact than the configuration of tangent spheres, so that the tangent-sphere configuration is then "outside" the saddle as regards compactness. Actually, at $(Z^2/A)_{\text{eff}} = (Z^2/A)_{\text{eff thr}}$, the tangent-sphere configuration has to be a little more compact than the saddle. This small extra compactness is then lost in the dynamical evolution of the nuclear configuration because, while the neck between the two spheres is growing, the electric repulsion begins to push the fragments apart. This is illustrated by the calculations in Ref. (1). In the model used there the saddle-point shape's compactness (as represented by its "block ratio", i.e. maximum elongation divided by the maximum transverse dimension) is equal to the compactness corresponding to tangent spheres at an effective fissility parameter x_{eff} equal to 2/3. [The effective

fissility parameter x_{eff} is approximately related to $(Z^2/A)_{eff}$ by $x_{eff} \approx (Z^2/A)_{eff}/47.$] Nevertheless, the actual dynamical calculations in Ref. (1) gave for the threshold of the effective fissility parameter x_{eff} the value 0.57 rather than 2/3. The difference $(2/3 - 0.57) \approx 0.10$ is associated with the extra compactness one must have in the initial tangent-sphere configuration in order to allow for the loss of compactness induced by the electric repulsion during the assault on the saddle-point.

Now, for the macroscopic saddle-point shapes calculated exactly, the value of x_{eff} where the saddle has the same block ratio as tangent spheres, is not 2/3 but 0.80 (see Fig. 4). Hence, an improved estimate of $x_{eff\ thr}$ might be

$$x_{eff\ thr} \approx 0.80 - 0.10 = 0.70 \quad ,$$

instead of

$$x_{eff\ thr} \approx 0.67 - 0.10 = 0.57.$$

Now $x_{eff\ thr} = 0.70$ corresponds to $(Z^2/A)_{eff\ thr} = 33.0$. It seems possible, therefore, that the difference between the estimate $(Z^2/A)_{eff\ thr} \approx 26\text{-}27$, obtained using the schematic model, and the value 33 ± 1, suggested by experiment, may be associated, at least in part, with the known shortcomings of that model in describing the static saddle-point configurations.

B. The thud wall slope coefficient a

A similar, but so far only qualitative, remark may be made concerning the difference between $a \approx 5$, suggested by Ref. (1), and $a = 12 \pm 2$, deduced from experiment. As seen from Fig. 4, the exact saddle-point configurations exhibit a rapid transition from necked-in shapes to cylinder-like shapes in the neighborhood of $x \approx 0.7$. This is a well-known phenomenon, first hinted at in the 1947 calculations of Frankel and

Metropolis[9] and since elucidated in several investigations[10]. (It is associated with an almost perfect cancellation, for $x \approx 0.7$, of the electric and surface tension forces for a wide range of configurations, leading to a plateau in the potential-energy landscape[10].) This rapid change in the elongation and neck radius of the true saddle-point shapes, seen in Fig. 4, is lost in the schematic model of Ref. (1), according to which the neck radius, for example, is just proportional to x. [A simple improvement in the treatment of the electrostatic energy appears to restore to the model some of the correct qualitative features of the saddle-point shapes--see Fig. 27 in Ref. (2).] The result is that if, in the theoretical calculations, the true saddle-point shapes had been used, the extra push needed when the effective fissility $(Z^2/A)_{eff}$ exceeded the threshold value would be a much steeper function of the excess over the critical condition than in the schematic model. A factor of two or more in the steepness coefficient a might well result, but whether quantitative agreement will, in fact, be obtained, remains to be seen.

C. The angular momentum fraction f

As can be seen from Fig. 3, the experimental trends, taken at face value, would probably not be reproduced optimally by either taking $f = 1$, corresponding to approaching spheres before contact, or $f \approx 0.54$, corresponding to the limit of rigidly stuck spheres with a ratio of masses of about 208:50. Dynamical model calculations of the clutching stage by G. Fai (private communication) should throw light on the question to what extent the use of a fixed effective angular momentum fraction f is appropriate and whether the value $f \approx 3/4$ is to be expected from the One-body Dissipation Theory.

V. THE EXTRA-EXTRA PUSH

Refs. (1,2) suggested the possible usefulness of making a distinction between fusion or mononucleus formation, involving the overcoming of the conditional saddle-point (the saddle-point at frozen asymmetry) and compound nucleus formation, involving the overcoming of the true (unconditional) saddle-point. The discussion in the preceding sections focused on the former, the extra injection energy underlying that discussion being the extra energy needed to overcome the conditional saddle. The first few fragmentary results on the "extra-extra push" needed to overcome the true saddle were presented in Ref. (1). More complete calculations are now available within the framework of the schematic model of Ref. (1) and will be described briefly in what follows.

Figure 5 shows, first, the result of a more recent calculation of the extra push, essentially the same as Fig. 13 in Ref. (1), except for two minor changes: the plot of the extra push is against Z_1, Z_2 rather than A_1, A_2, and the nuclear parameters differ a little from those used in Ref. (1), with the result that $x_{\text{eff thr}}$ is now 0.584 rather than 0.57. The contour lines in Fig. 5 follow loci of equal values of $(Z^2/A)_{\text{eff}}$.

Figure 6 shows contour lines of the extra-extra push. For symmetric systems (along the diagonal line $Z_1 = Z_2$) and in the region marked "beach", below the "cliff", the extra-extra push is the same as the extra push. Above the cliff (which in the schematic model turns out to be an almost vertical one) the extra-extra push is higher than the extra push. The height of the cliff, which is a little under 10 MeV for very asymmetric systems gradually diminishes as one moves toward symmetry, fading away entirely at symmetry. Thus, the extra-extra push, needed to make a compound nucleus, is never less than the extra push to make a mononucleus (fusion). For heavy asymmetric systems it is often much higher.

We hope to come back to a fuller discussion of these calculations at a later date and to a comparison with experimental results, especially on measurements of evaporation-residue cross-sections. Here we shall just mention two points. First, a reminder that the theoretical results are based on the schematic model of Ref. (1) and they are, therefore, at best, qualitative. For a quantitative comparison with experiment a more refined calculation will be needed. Alternatively, the structure of the qualitative results might be accepted, with relevant parameters of the theory extracted by comparisons with experiments, along the lines of the discussion of the extra push given in this paper.

Second, a qualitative comment on the question of super-heavy element production. As can be seen from Fig. 6, the formation of a super-heavy compound nucleus out of two comparable pieces is opposed, in the present model calculations, by a huge "thud wall". The height of the thud wall decreases with increasing asymmetry and even disappears entirely, but only for very asymmetric target-projectile combinations that would appear to be difficult to achieve in realistic experiments.

VI. THE SUPERFLUID SLITHER AND THE SUPERVISCID SHOVE

We will end with a speculation associated with an obvious limitation of the present discussion, which is based on the dissipation-dominated (superviscid) One-body Dissipation Dynamics.

Nuclei in their ground states exhibit striking pair-correlation effects, closely related to the phenomena of superfluidity and superconductivity in macroscopic bodies[11]. These effects are expected to be destroyed by an excitation energy of several MeV (a few times the pair correlation energy), at which point something like a phase transition to a

normal state would be expected to take place[12]. According to the One-body Dissipation theory this normal state is expected to be dominated by dissipation (apart from shell effects): it is a superviscid state. Now in many nucleus-nucleus collisions the initially cold, (pseudo-) superfluid nuclei will often become excited to well over 10 MeV soon after contact, so superfluidity should, perhaps, give place rather suddenly to superviscidity. How would one look for evidence of such a superfluid-superviscid transition?

As we have seen above, one of the straightforward predictions of the one-body theory of superviscid nuclear dynamics is the need to provide a very substantial extra push in order to make two sufficiently heavy nuclei fuse. But superviscidity is not expected to operate (at least not for a while) when two cold nuclei are brought into gentle contact, using a bombarding energy within a few MeV of the interaction barrier. Under such conditions a large extra push might not be necessary for fusion. It follows that at energies close to the interaction barrier two nuclei might have a better chance to fuse than either well below the barrier (obviously!) or somewhat above, when superfluidity has been destroyed but the energy may still be below the dynamical threshold for fusion. This argument suggests that, under suitable conditions, one might look for a maximum in the primary fusion cross-section around the interaction barrier, followed, at still higher enegies (exceeding the dynamical threshold) by a renewed rise. (This prediction refers to the fusion cross-section or to the primary compound-nucleus cross-section, before fission and particle emission.)

Thus, for systems with $(Z^2/A)_{eff}$ exceeding the threshold value, there might begin to appear two distinct ways of achieving fusion or compound-nucleus formation: a Superfluid Slither in the immediate vicinity of the interaction barrier and the Superviscid Shove when the extra-push energy has been supplied.

The possible existence of two mechanisms for collective shape changes in the context of fission had been considered in the past, especially by L. Wilets[13]). In particular, the discussion of the flow of probability between pairs of near-crossing levels in a system reveals the two limits of adiabatic and diabatic behavior. The adiabatic (low-dissipation) behavior would be enhanced by pairing (superfluidity) but it might be in evidence, at sufficiently low rates of deformation, even in the absence of pairing[14]). In such cases the term "Adiabatic Slither" would seem more appropriate than "Superfluid Slither". [In this connection see also Figs. (13-16) in Blocki, et al.[3]), which illustrate the large deviations from the wall-formula dissipation that are to be expected--especially at low rates of deformation--when symmetries are present and the concept of level crossings or near-crossings becomes relevant.]

ACKNOWLEDGMENTS

I would like to thank the authors of Ref. (4) for making available their experimental results before publication and especially Sven Bjørnholm and Henning Esbensen for enlightening discussions and very valuable correspondence.

This work was done in the Nuclear Science Division of the Lawrence Berkeley Laboratory and supported by the Director, Office of Energy Research, Division of Nuclear Physics of the Office of High Energy and Nuclear Physics of the U.S. Department of Energy under Contract W-7405-ENG-48.

REFERENCES

[1] W.J. Swiatecki, "The Dynamics of Nuclear Coalescence or Reseparation", talk presented at the Nobel Symposium on High-Spin States, Örenäs, Sweden, June 22-25, 1980, to be published in Physica Scripta, 1981; Lawrence Berkeley Laboratory preprint LBL-10911. For earlier estimates of an extra push see also J.R. Nix and A.J. Sierk, Phys. Rev. C15, 2072 (1977).

[2] W.J. Swiatecki, Prog. Particle & Nucl. Phys. 4, 383 (1980); Lawrence Berkeley Laboratory preprint LBL-8950, March 1979.

[3] J. Randrup and W.J. Swiatecki, Annals of Phys. 124, 193 (1980); J. Blocki, Y. Boneh, J.R. Nix, J. Randrup, M. Robel, A.J. Sierk, and W.J. Swiatecki, Annals of Phys. 113, 338 (1978).

[4] H. Sann, S. Bjørnholm, R. Bock, Y.T. Chu, A. Gobbi, E. Grosse, U. Lynen, E. Morenzoni, W. Müller, A. Olmi, D. Schwalm, and W. Wölfli, "Fusion Reaction Studies of Transuranic Nuclei", Proc. Int. Conf. on Nuclear Physics, Aug. 24-30, 1980, Berkeley, California, Lawrence Berkeley Laboratory report LBL-11118; A. Gobbi, Contribution to "GSI Nachrichten" 1-81, p. 4, 1981; H. Sann, R. Bock, Y.T. Chu, A. Gobbi, A. Olmi, U. Lynen, W. Müller, S. Bjørnholm, and H. Esbensen, "Deformability as a Critical Factor in Initiating Fusion between Very Heavy Ions", GSI-Preprint 81-6, February 1981, submitted to Phys. Rev. Letters.

[5] R. Bass, Nucl. Phys. A231, 45 (1974).

[6] J. Blocki, J. Randrup, W.J. Swiatecki and C.F. Tsang, Annals of Phys. 105, 427 (1977); J. Blocki and W.J. Swiatecki, "A Generalization of the Proximity Force Theorem", Lawrence Berkeley Laboratory preprint LBL-9574, August 1980, to appear in Annals of Phys., March 1981.

[7] L.C. Vaz, J.M. Alexander and G.R. Satchler, "Fusion Barriers, Empirical and Theoretical: Evidence for Deformation in Subbarrier Fusion", Phys. Reports 1981, in press.

[8] F. Beck, J. Blocki, M. Dworzecka and H. Feldmeier, preprint IKDA 80/9, August 1980, to be published; H. Feldmeier, Nukleonika 25, 171 (1980); J. Blocki, F. Beck, M. Dworzecka, and H. Feldmeier, Proc. Int. Workshop on Gross Properties of Nuclei and Nuclear Excitations VIII (1980) p. 157; F. Beck, J. Blocki, M. Dworzecka, and G. Wolschin, Phys. Lett. 76B, 35 (1978); J. Blocki and W.J. Swiatecki, "Nuclear Deformation Energies", in preparation.

[9] S. Frankel and N. Metropolis, Phys. Rev. 72, 914 (1947), especially Fig. 8.

[10] S. Cohen and W.J. Swiatecki, Annals of Phys. 19, 67 (1962), especially Figs. 24, 26, 29 and 30; Annals of Phys. 22, 406 (1963), especially Figs. 1 and 2.

[11] A. Bohr and B.R. Mottelson, "Nuclear Structure", W.A. Benjamin, Inc., 1975, especially Volume II, p. 395.

[12] C. Yannouleas, M. Dworzecka, and J.J. Griffin, Nucl. Phys. A339, 219 (1980).

[13] L. Wilets, Theories of Nuclear Fission, Oxford, Clarendon Press, 1964.

[14] The author is indebted to Prof. W. Nörenberg for discussions in which he stressed this point.

FIGURE CAPTIONS

Fig. 1. The cross-section for bringing two idealized nuclei into contact is shown by the solid curves. For systems with an effective fissility $(Z^2/A)_{eff}$ below the threshold value (Fig. 1a) it is also the fusion cross-section, from the interaction barrier E_B up to a center-of-mass energy exceeding the barrier by $(-c_1)/c_2$. At higher energies the fusion cross-section falls below the standard formula, as shown by the dashed curve. For sytems with $(Z^2/A)_{eff}$ greater than the threshold value (Fig. 1b), the fusion cross-section does not begin its main rise until the energy has exceeded the interaction barrier by c_1^2. [This is looking apart from (small) subthreshold effects, which may include barrier penetration, fluctuations or a "Superfluid Slither", suggested in Section VI.]

Fig. 2. Comparison of experimental fusion cross-sections (associated with outgoing fragment masses centered around symmetry) with theory. The solid curves are conventional reaction cross-section predictions and the dashed curves incorporate the requirement of an extra push in the approach degree of freedom. [I deduced the data points from Ref. (4) and added purely nominal 10% error bars.]

Fig. 3. In (a) the quantity F, proportional to the square root of the cross-section defect, is plotted aginst X, proportional to the energy-weighted reduced cross-section. The symbols identify the reactions according to the same key as in Fig. 1. The theory corresponds to the parallel lines. Their intercepts on the F-axis, marked by dots, are plotted against $(Z^2/A)_{eff}$ in Fig. 3b. The resulting straight line defines the threshold value $(Z^2/A)_{eff\ thr}$ (marked by a star) and its slope is the thud wall slope parameter a.

Fig. 4a. The "block ratio" (maximum length divided by maximum transverse dimension) for unconditional saddle-point shapes is plotted against the fissility parameter x. [The behavior of conditional saddle-point shapes in their dependence on the effective fissility parameter x_{eff} may be deduced using the static scaling rule of Ref. (1).] The solid line corresponds to exact calculations [e.g. Ref. 10)]. The dashed line is deduced from Ref. (1). (Its equation is $1 + \sqrt{1 + 2x - 3x^2}$.) The block ratio for tangent spheres is 2, and this value is recrossed by the dashed curve at x = 2/3 and by the solid curve at x = 0.80. In this region of x-values the rate of contraction of the exact shapes is much more rapid than of the model shapes.

Fig. 4b. The minimum transverse dimension (i.e. the neck diameter) divided by the maximum transverse dimension, for unconditional saddle-point shapes, is plotted as a function of the fissility parameter x. The exact saddle-point shapes (solid curve) show a very rapid transition from necked-in to cylinder-like shapes near $x \approx 0.7$. This feature is lost in the schematic model (dashed line), according to which $(R_{min}/R_{tr}) = x$.

Fig. 5. Contour lines (in MeV) of the estimated extra push over the interaction barrier, needed to overcome the conditional saddle (i.e. the saddle at frozen entrance-channel asymmetry) and achieve fusion in a head-on collision. The results follow from solving eqs. (23,24) in Ref. (1), with slightly different nuclear parameters than used there. Below the zero-push contour, corresponding to $x_{eff} = 0.584$, fusion follows automatically after contact. The plot is against the atomic numbers Z_1 and Z_2 of the two colliding nuclei. The combined system $Z_1 + Z_2$ is always assumed to be on the valley of beta stability, as approximated by Green's formula: $N - Z = 0.4A^2/(200 + A)$.

Fig. 6. Contour lines (in MeV) of the estimated "extra-extra push" over the interaction barrier, needed to overcome the unconditional saddle and to form a compound nucleus if it exists (i.e. if the fissility parameter x is less than one) or to achieve a spherical configuration if it does not (i.e. if $x > 1$). The results were obtained by solving the equations of motion which follow from Ref. (1), with the asymmetry degree of freedom unfrozen in the mononuclear regime. Note the peculiar cliff (almost vertical in the schematic model) above which the extra-extra push is greater than the extra push in Fig. 5.

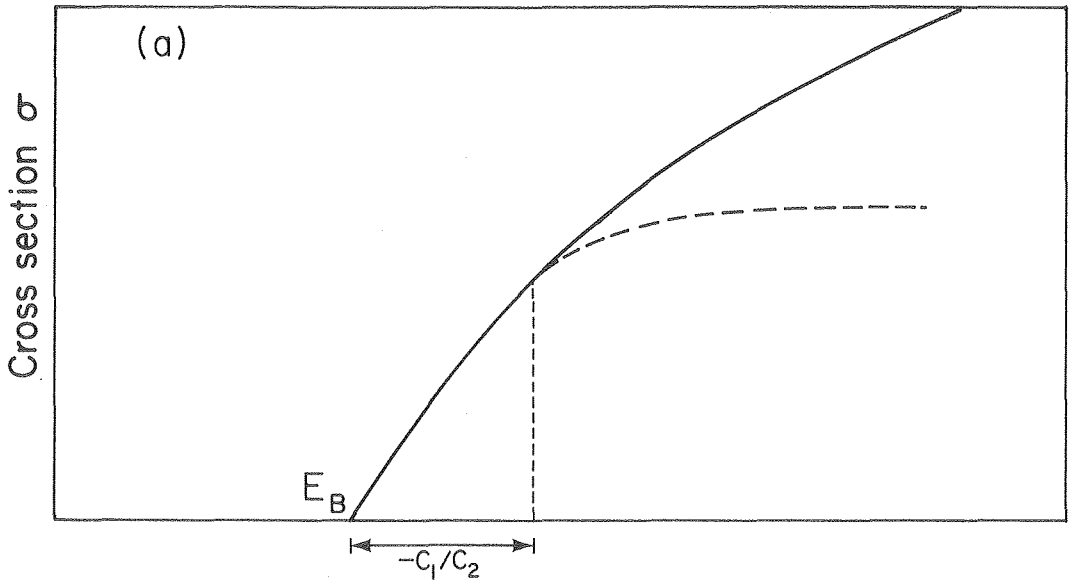

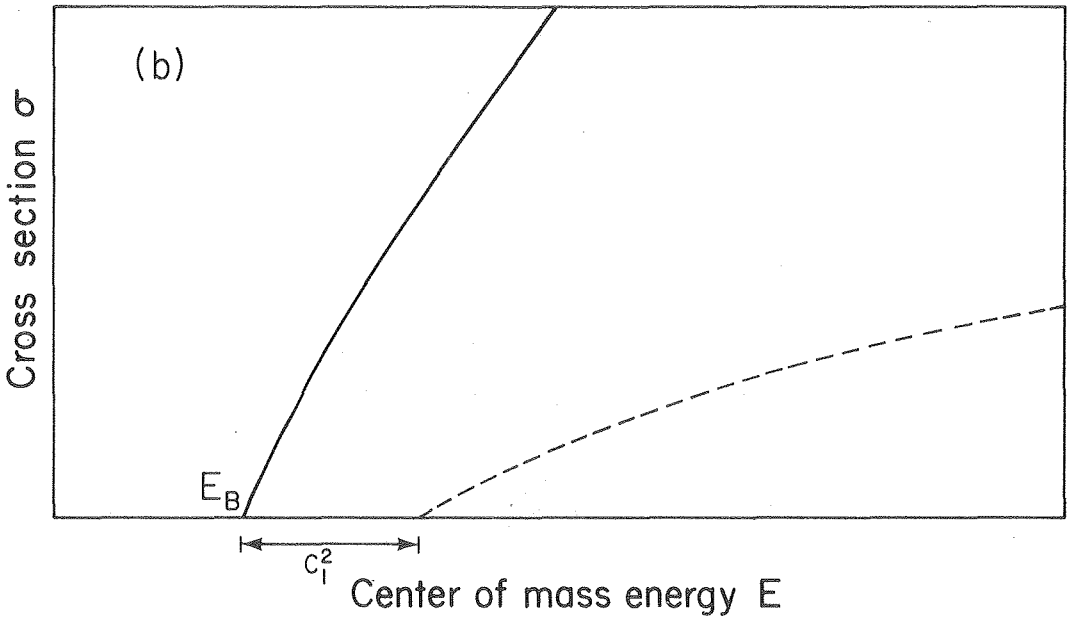

Solid line : $\sigma = \frac{\pi r_c^2}{E}(E - E_B)$

Dashed line : $\sigma = \frac{\pi r_c^2}{E}\left[\sqrt{\left(\frac{C_1 C_2 + 1/2}{C_2^2}\right)^2 - \left(\frac{C_1^2 + E_B - E}{C_2^2}\right)} - \left(\frac{C_1 C_2 + 1/2}{C_2^2}\right)\right]$

XBL 815-835

Fig. 1

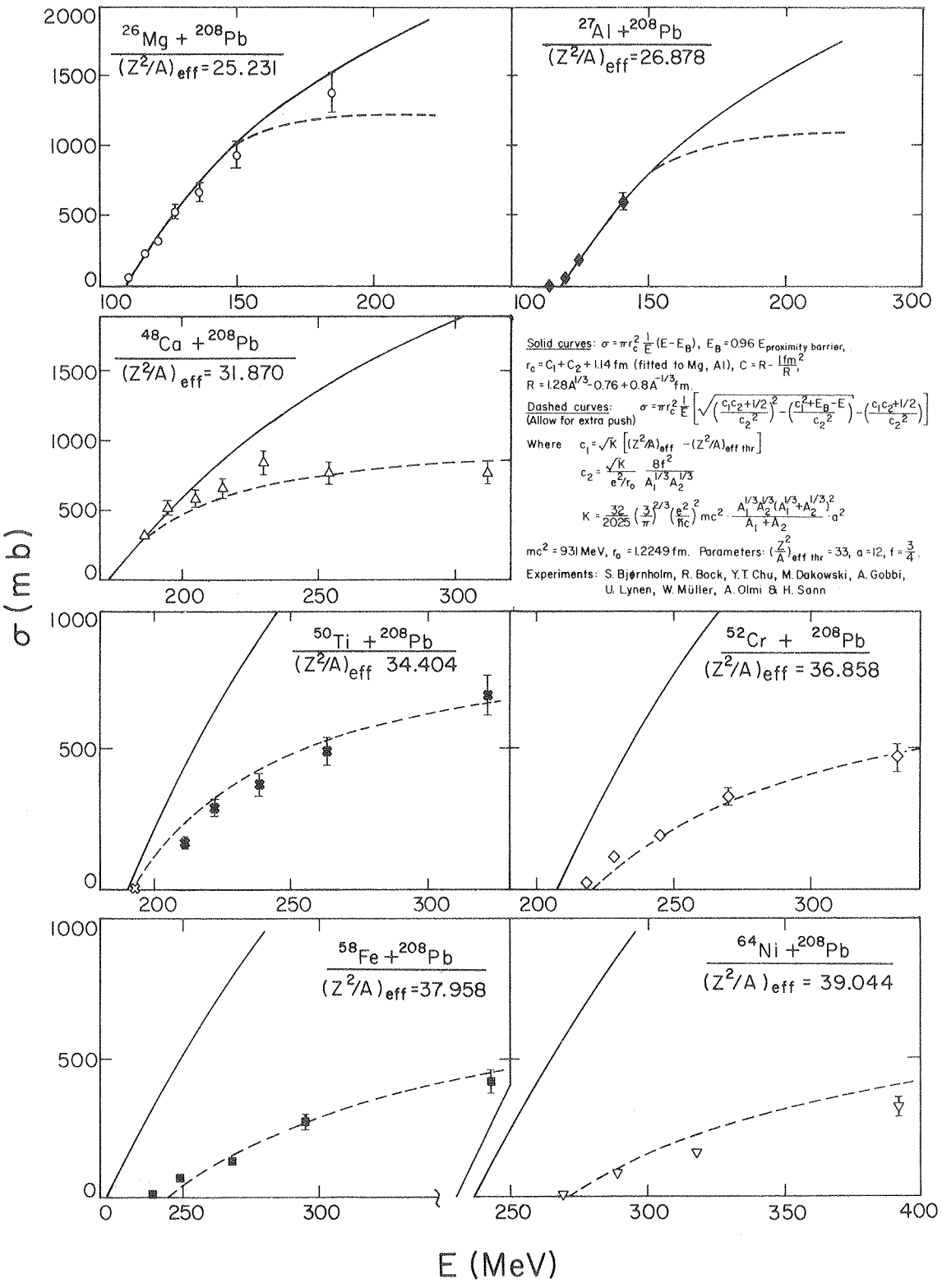

XBL 815-829

Fig. 2

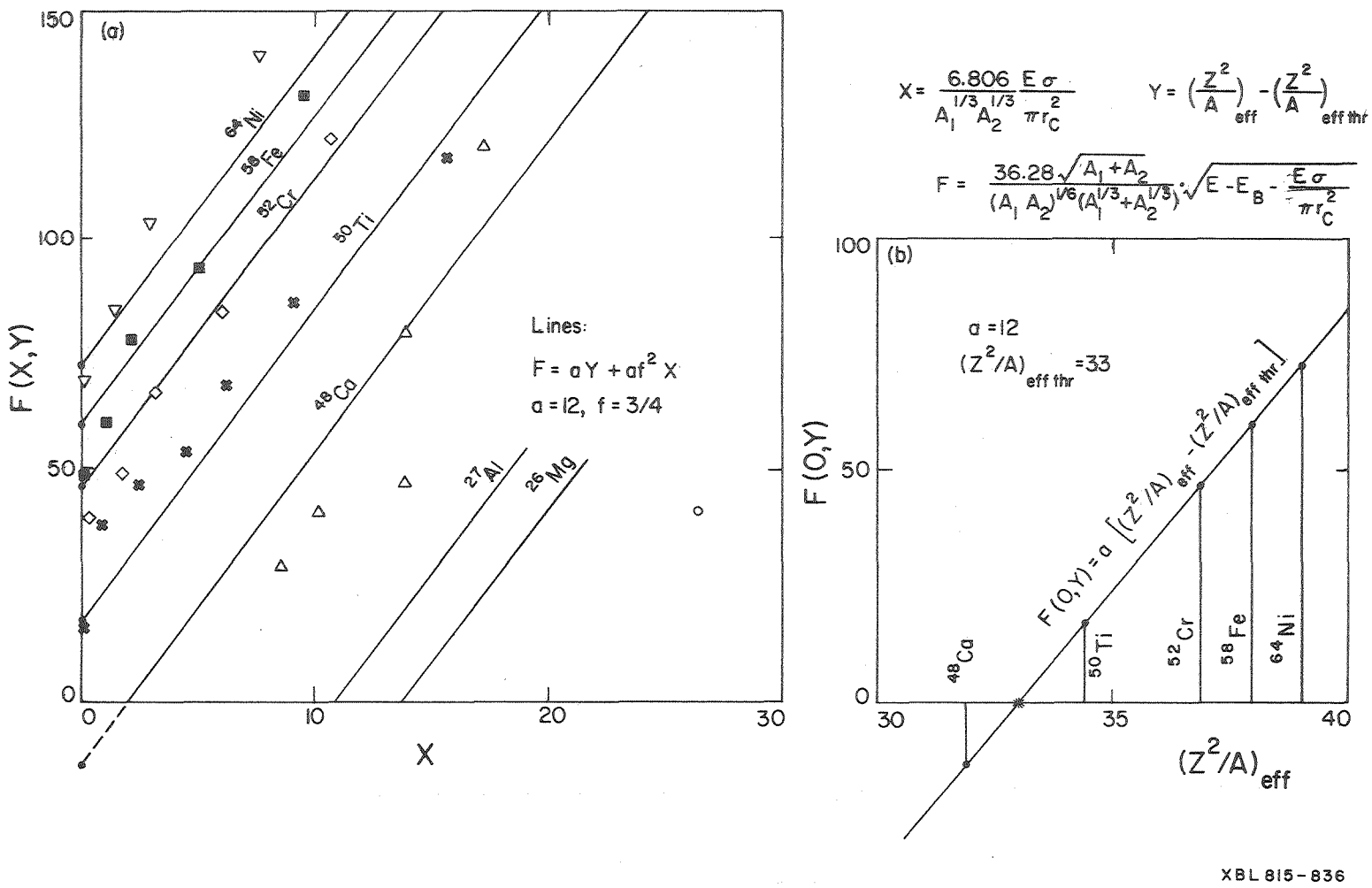
(a)
F(X,Y)
X
64Ni
58Fe
52Cr
50Ti
48Ca
27Al
26Mg
Lines:
F = aY + af² X
a = 12, f = 3/4
X = 6.806 E σ / A1^1/3 A2^1/3 π r_c²
Y = (Z²/A)_eff − (Z²/A)_eff thr
F = 36.28 √(A1+A2) / (A1 A2)^1/6 (A1^1/3+A2^1/3) · √(E − E_B − E σ / π r_c²)
(b)
a = 12
(Z²/A)_eff thr = 33
F(O,Y) = a [(Z²/A)_eff − (Z²/A)_eff thr]
F(O,Y)
(Z²/A)_eff
48Ca
50Ti
52Cr
58Fe
64Ni
XBL 815-836

Fig. 3

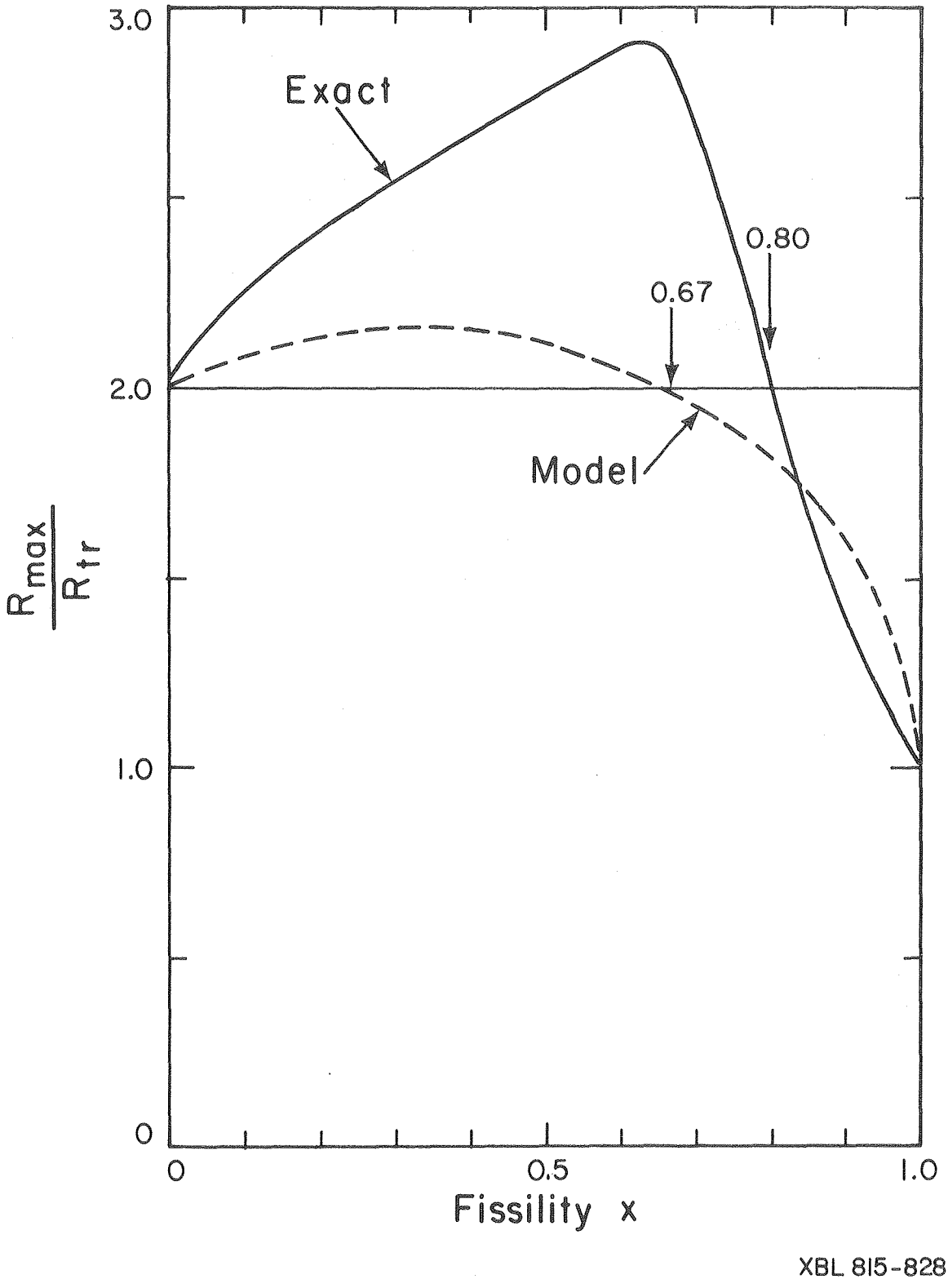
3.0
2.0
1.0
0
Exact
0.80
0.67
Model
$\frac{R_{max}}{R_{tr}}$
0
0.5
1.0
Fissility x
XBL 815-828

Fig. 4a

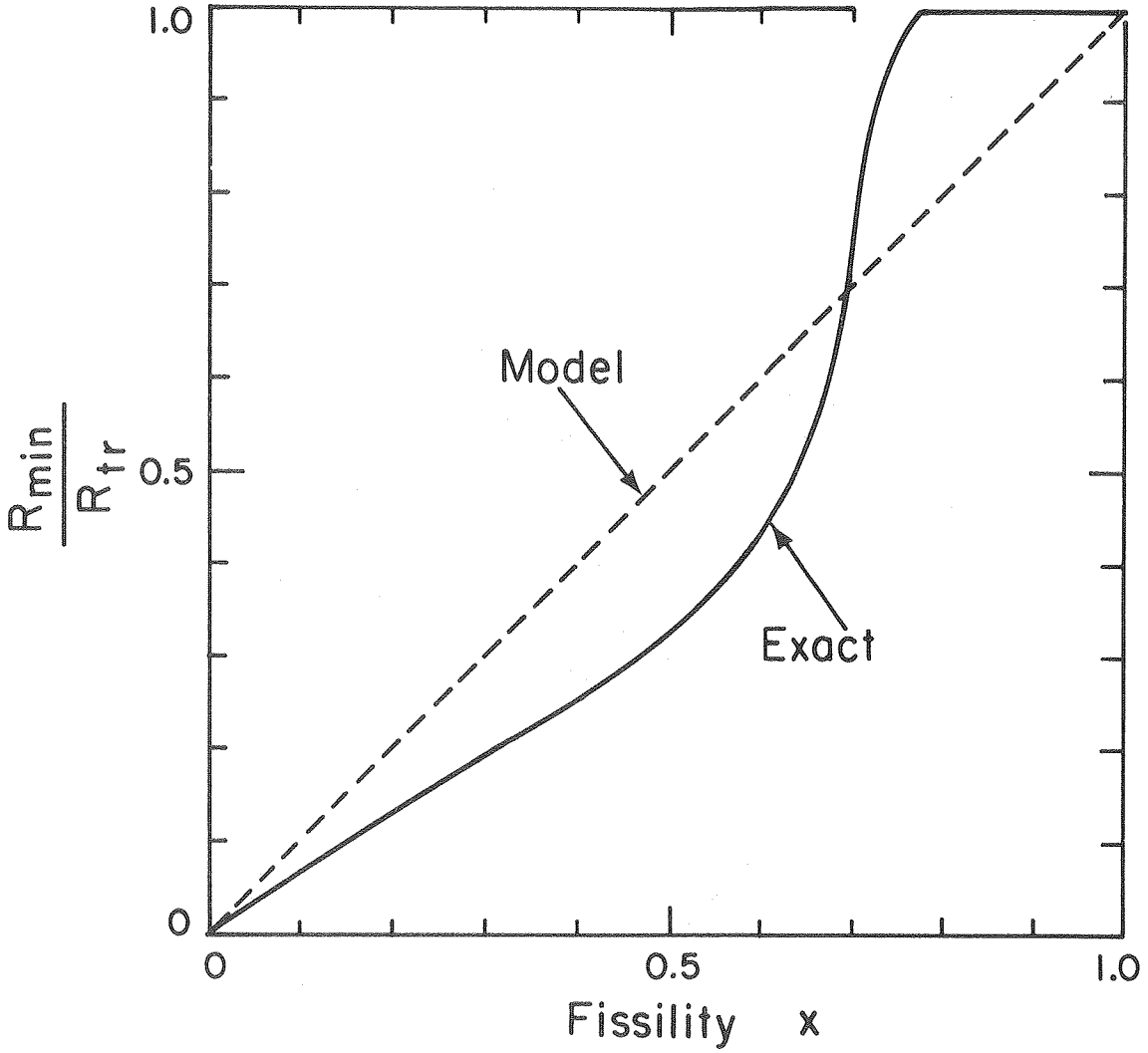
1.0
0.5
0
$\frac{R_{min}}{R_{tr}}$
Model
Exact
0
0.5
1.0
Fissility x
XBL 815-827

Fig. 4b

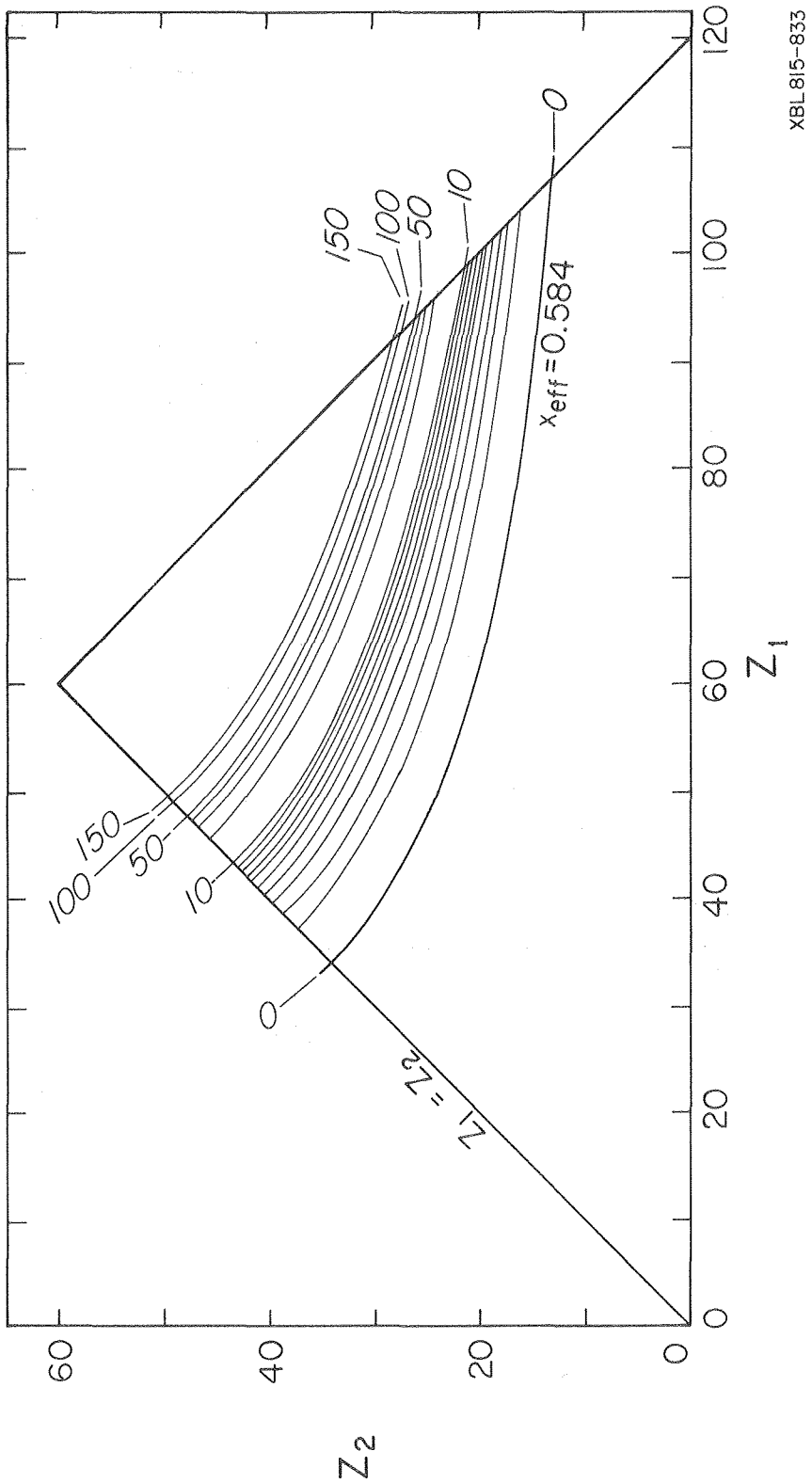

XBL815-833

Fig. 5

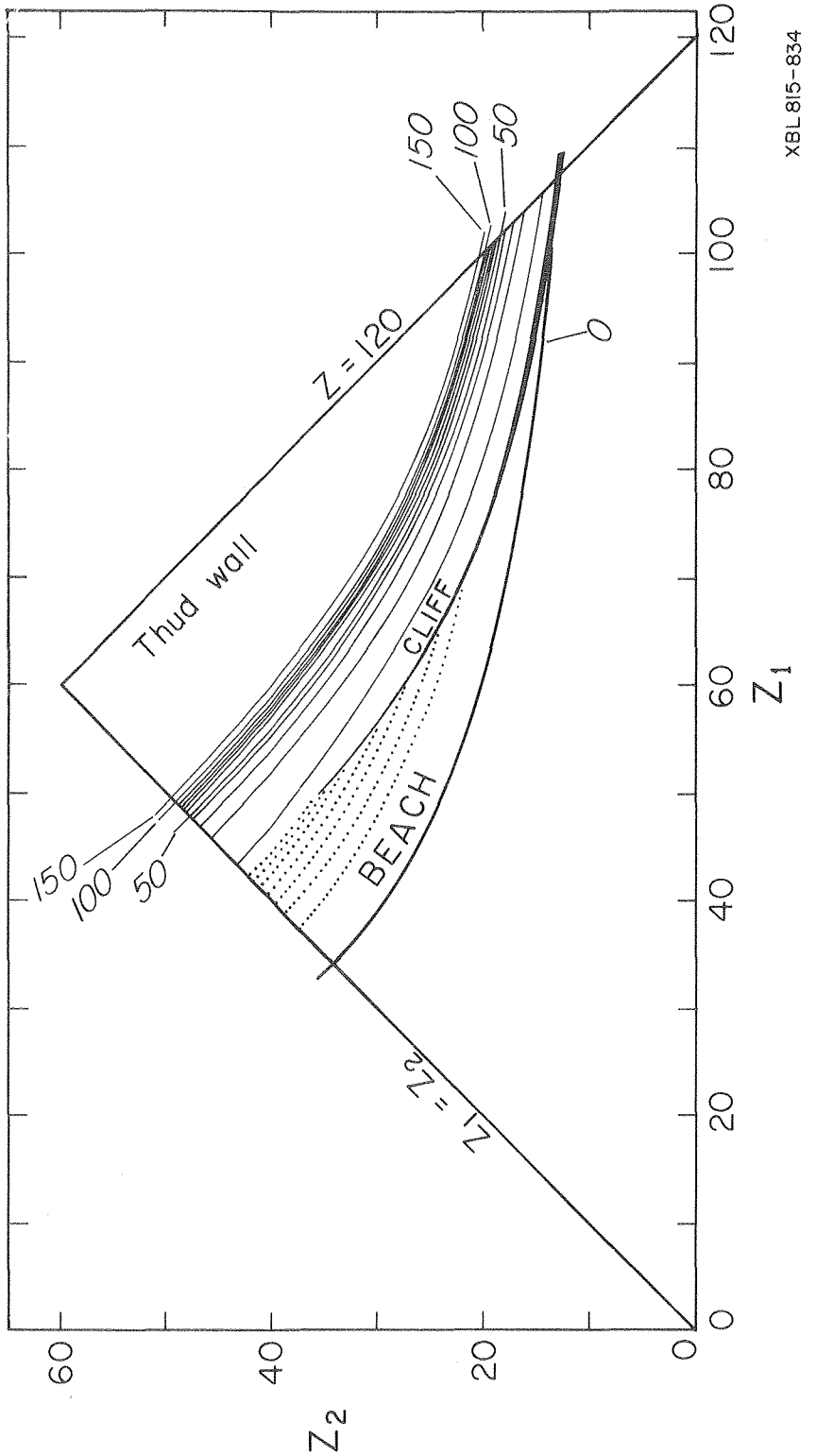
Thud wall
Z = 120
150
100
50
0
CLIFF
BEACH
150
100
50
Z = Z2 - Z1
0
20
40
60
80
100
120
Z1
0
20
40
60
Z2
XBL 815-834

Fig. 6